

1 **Non-destructive method for the identification of ceramic production**
2 **by portable X-rays Fluorescence (pXRF).**

3 **A case study of amphorae manufacture in central Italy**

4
5 Letizia Ceccarelli^{1,*}, Ilenia Rossetti², Luca Primavesi², Simon Stoddart¹

6 ¹ University of Cambridge, McDonald Institute for Archaeological Research, Downing Street
7 Cambridge CB2 3ER, UK

8 ² Dip. Chimica, Università degli Studi di Milano, via C. Golgi 19, 20133 Milano, Italy

9
10
11 **ABSTRACT**

12 Portable X-rays Fluorescence (pXRF) represents one of the most effective tools for in situ,
13 non-destructive elemental analysis, which has a valuable application in the study of ceramic
14 production. However, whilst the qualitative assessment of the composition of artefacts is
15 reliable, the quantitative analysis can be biased by some limitations, due to instrumental
16 features or materials properties. The analysis of ceramic materials is particularly challenging
17 due to the lack of representative calibrations and standards, as well as the low density and
18 poor homogeneity of samples. In this contribution, a method is proposed to fingerprint a
19 ceramic production through pXRF analysis. At the site of Montelabate (Perugia) in central
20 Italy four kilns were excavated revealing a production of amphorae. This site was therefore
21 selected as a suitable case study for fingerprinting a ceramic production. After qualitative
22 analysis, representative calibration standards were created based on different commercial
23 clays and feldspars. These can help overcoming the well-known matrix effect, both physical
24 and chemical, and may offer a representative and reproducible standard to be used in
25 different laboratories.

26 Alongside the precise assessment of composition, the possibility to fingerprint a
27 production was also assessed using a different method, based on the intensity ratio between
28 selected elements. The relevant elements were chosen based on their correlation and non-
29 correlation. Correlated elements were attributed to the raw clay used for ceramic production

* Corresponding author: Letizia Ceccarelli lc368@cam.ac.uk

30 and non-correlated elements were attributed to the specific fabric recipe. Accordingly, some
31 benchmarks to identify the clays and fabric used in the site of Montelabate were identified.
32 Amphorae found at other ancient commercial sites in the area of Rome were therefore also
33 compared with these benchmarks in order to assess their provenience.

34

35 *Keywords:* X-rays Fluorescence; Ceramic analysis; Fingerprinting a production; Amphorae
36 analysis; Montelabate; Central Italy manufacture.

37

38 **1 - INTRODUCTION**

39 X-rays Fluorescence (XRF) is an analytical technique widely applied in archaeology for
40 decades and the development of portable instruments allowed increasingly fast applications
41 to analyse the elemental composition of archaeological material (Schackley 2011, Frahm and
42 Doonam, 2013, Shugar and Mass 2014).

43 XRF is a non-destructive procedure which offers information on the chemical
44 composition of samples, relying on its bulk elemental composition and not specifically
45 sensitive to the surface. The use of a portable device, as in this case, additionally permits fast
46 analyses in the field, requiring only a quick and standard setup to collect data. Therefore it
47 can be conveniently adopted for routine analysis to correlate pottery productions and to
48 confirm, or exclude, identifications based primarily on macroscopic observations.

49 The successful application of XRF analysis on ceramic elements and the results of the
50 collected data has been widely debated (Hunt and Speakman, 2015; Speakman et al., 2011).
51 Central to the debate is that ceramics have a lower density than metals and therefore scatter
52 more effectively radiation, which may limit to some extent the sensitivity of the analysis.
53 Typically, the lower detection limit for XRF is tens of ppm, but it requires longer spectra
54 collection time and the absence of any interfering element. Some limitations are also
55 intrinsically correlated to the type of analysis, which suffers of the so-called “matrix effect”.
56 Instances in which it is necessary to obtain highly accurate quantitative analysis at low
57 concentrations of critical light elements may require vacuum analysis as the surrounding air
58 absorbs the lower energy X-rays generated by the excitation of low-Z elements. Therefore, it
59 is often misleading to look at quantitative results of the order of few ppms: this is not a very
60 sensitive analytical tool, as also noted by (Hunt and Speakman, 2015, 637).

61 A further critical point is based on the variable total intensity of spectra collected over
62 different samples with identical composition, depending on scattering and on possible
63 fluctuating intensity of the source, which often make quantitative analysis with absolute
64 values unreliable. Indeed, the intensity of the whole spectrum seems to sometimes vary. The
65 data should be compared (and in each case normalised) with repeated measurements of a
66 standard or calibration sample, to check reproducibility.

67 Additionally, XRF incident radiation has limited penetration so that elements that are
68 more abundant on the surface are predominantly detected, which may be significantly
69 different from the bulk composition of a sample. This is particularly relevant when it is
70 impossible to obtain a homogeneous sample through grinding or melting. It should also be
71 noted that when using factory calibration through commercial algorithms, relative errors
72 around 50% may be even achieved, while custom standardisation typically induces a relative
73 error of less than 10%.

74 As previously noted, there has been extensive discussion of the error sources during
75 quantitative XRF analysis of ceramics which have been reviewed by Speakman and Shackley
76 2013 and by Conrey et al., 2014, specifically focused on the archaeological application of this
77 analytical method. These contributions also suggest procedures and calibration methods to
78 avoid severely misleading results. It is clear from these studies that the use of commercial or
79 automatic calibration software, as well as that of raw intensity data, must be carefully
80 avoided. Furthermore, factory calibrations for ceramics and obsidian, the materials most
81 intensively studied in this field, do not exist. Factory-installed calibrations are not adequate
82 for quantification of elements in non-metallic archaeological materials (Speakman et al.,
83 2011). A more positive stance on the application of pXRF on ceramics has been provided by
84 (Attaelmanan and Mouton, 2014). The conclusion is that some of the limitations, amongst
85 which are those described above, can be overcome by combining different analytical tools. It
86 is apparent that the correct set up of an analysis protocol for data collection and interpretation
87 can resolve most of the issues above described.

88 This paper presents an analytical method based on pXRF for the identification of
89 ceramic fabrics and provenance identification. The results presented here are part of the
90 FABRICS project, established between the McDonald Institute for Archaeological Research
91 at Cambridge University and the Department of Chemistry of the Università degli Studi di
92 Milano, which aims to develop an integrated methodology to fingerprint ceramics production.
93 The techniques employed include portable X-ray fluorescence (pXRF) and Fourier Transform

94 Infrared Spectroscopy (FT-IR) for compositional data, while structural data are collected by
95 X-Ray Diffraction (XRD) and Near-Infrared spectroscopy (NIRS).

96 This study aims to establish a standard non-destructive methodology to fingerprint pottery by
97 pXRF, allowing the scientific classification of artefacts, using as a case study the unique
98 discovery of four pottery kilns excavated in 2012 in central Italy at Montelabate (Perugia,
99 Italy), in the framework of the Montelabate Project (under the direction of Simon Stoddart
100 and Caroline Malone). The workshop, in use from the 1st century AD to the late 4th –early 5th
101 century AD producing amphorae then later courseware, offers the perfect model for the study
102 of the technique of production.

103

104 **2 – THE CASE STUDY**

105

106 **2.1. Ceramic production**

107 One of the earliest human skills was in crafting a range of clay objects. It is fundamental to
108 understand the development of the technical processes of manufacture in antiquity as it can
109 be seen as a foundation of the modern industrial process. Traditionally, archaeology classifies
110 the development of technology on the basis of the evolution of objects and the identification
111 of similar fabrics is performed on the basis of the colour of clay and its composition, however
112 such observations can be misleading. Colour may vary due to organic impurities, leading to a
113 brown or black clay colour, or to transition metal ions. Iron in variable amounts and/or
114 oxidation leads to brown, red or yellow, whereas manganese usually leads to grey/green
115 colour, which is also typical of partially reduced iron (ferrous compounds).

116 The composition and oxidation state of some elements in the final ceramic may vary
117 depending on the thermal treatment in different sections. For instance, if a brown colour is
118 imparted by carbon residue, firing may eliminate them from the surface, but less effectively
119 from the inner part of the object, and this may be evidenced in a freshly broken section.
120 Similarly, a light red/brown colour is due to ferric oxide (*i.e.* oxidised iron ions), whereas
121 firing under reducing conditions, with limited air feed, may turn the surface greyish, leaving
122 the section with the original red/brown colour.

123



124

125 **Fig. 1:** Example of an object's section with different colours.

126

127 Temper is often added to impart specific properties. Calcium oxide can be added as a
128 fluxing agent, usually obtained through the decomposition of limestone and other carbonates.
129 The same function may be exerted by feldspars, which are stable in the temperature range of
130 firing between 700°C and 900°C. Non plastic materials, typically coarser than the clay, are
131 used to avoid excessive shrinkage during drying and firing. This is particularly important
132 when fine grains are used for the clay, which make the escape of water harder from inner
133 layers after the surface has dried. Coarser particles leave space for water to diffuse more
134 effectively towards the surface. Different rocks may be used, such as basalts, ardesites,
135 volcanic ash, glass or tuff. Sedimentary material may also be included, such as sandstone,
136 limestone and dolomite, or diatomaceous earth.

137 Finally, surface finishing is carried out to remove irregularities. In some instances a
138 suspension of clay in water is used for finishing, which may lead to some differences between
139 the surface and the bulk compositions. Therefore, it can be seen that is crucial to identify the
140 technical process of pottery production through the application of an integrated method of
141 analysis¹.

142

143

144

145

¹ An interesting approach to determine pottery fabric technology has been developed by the Groningen Institute for Archaeology (GIA) Laboratory for Conservation and Material Studies. It undertakes the classification of fabrics through the optical analysis of the compositional characteristics in fresh breaks in the pottery and by the re-firing of selected material at 600°C, 800°C and 1050° in an oxidising kiln in order to establish the firing characteristics of the material (Attema et al., 2003). However, no specific analytical method was employed in this study.

146 **2.2. The site**

147

148 The site of Montelabate is situated in the Upper Tiber valley, 30 km from Perugia, in
149 a valley characterised by a series of gentle hills 250-300m above sea level. The valley is
150 overlooked by the Abbey of S. Maria di Val dipone, today owned by the Gaslini Foundation,
151 in an area known for pottery production until the early 20th century.

152 Geologically, the valley is in the plain of the Umbrian basin delimited by lower hills
153 to the east separating it from the valley of Gubbio which is composed of Mesozoic-Tertiary
154 and Marly limestone (Malone and Stoddart, 1994, 17). The territory of Montelabate
155 comprises the catchment of a series of small rivers running south west flowing into the River
156 Tiber.

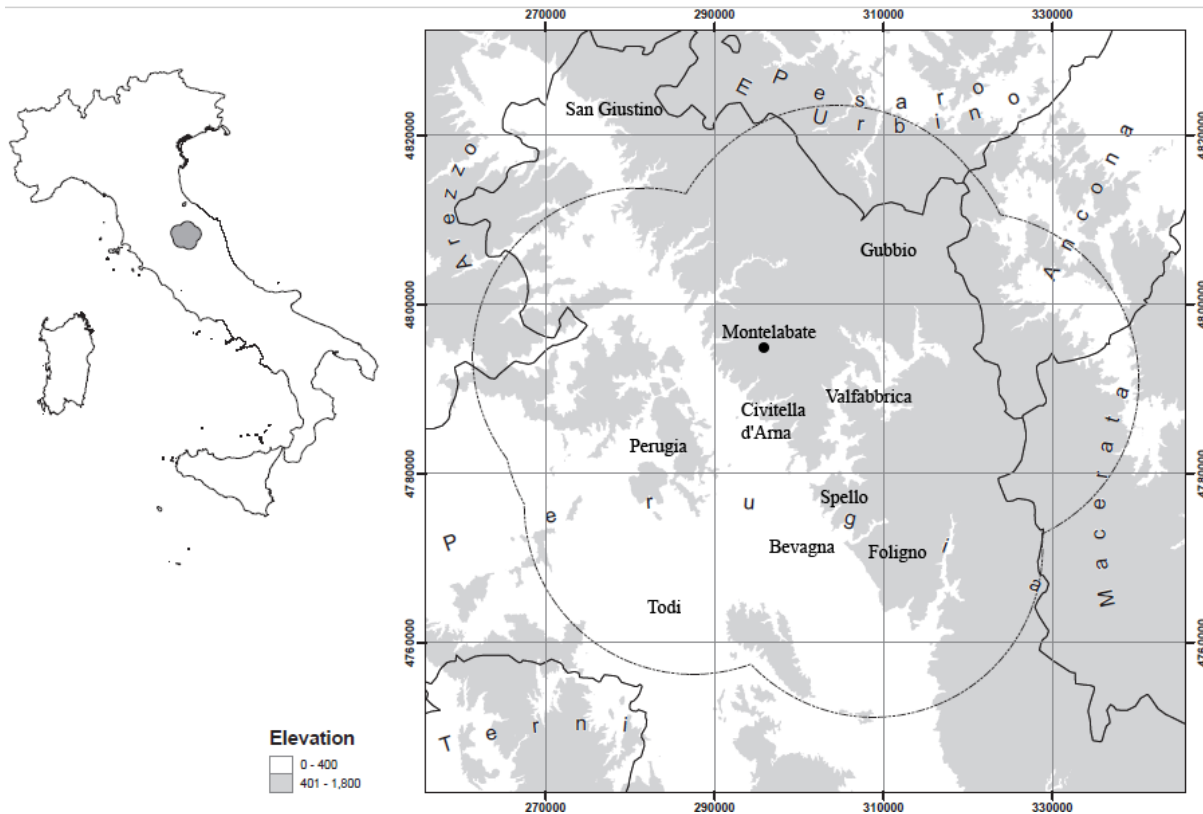
157 The production site, used as key-study in this study, for pottery manufacturing used
158 the Plio-Pleistocene clay deposits which are derived from the ancient Tiber basin, as the area
159 is characterised by a series of lithostratigraphic units and alternating alluvial sandy-clay
160 layers, created by water courses running into the lake that later become the River Tiber,
161 interbedded with calcareous and travertine gravels². The pottery manufacture is located in
162 walking distance to a rich clay deposit³ and both the river connectivity by the Ventia, a
163 tributary to the Tiber at a distance of 5km, and the densely forested hills surrounding the site
164 (Umbria was rich in forests as attested by Cic. Div. 1. 94) were the ideal combination for the
165 exploitation of local resources for production⁴.

166 An initial field walking survey conducted in 2010 (Stoddart et al., 2012) revealed an
167 interesting spatial patterning in the valley in the Roman period: rural settlements filled the
168 area, distributed both in the lower sandstone foothills between 250 and 300m above sea level,
169 on the Pliocene lacustrine sediments and on the terraces of the Tiber tributaries. The evidence
170 of the agricultural exploitation and the production of wine in the area are documented by a
171 complex kiln site, excavated in 2012, formed of three kilns and a workshop.

² For the area of Montelabate and the Tiber Valley (Beneduce and Lapadula 1997, 318-319). For Gubbio Bertacchini 2008, see also (Donnini and Rosi Bonci, 2008, 2-3).

³ The application of Near-Infrared Spectroscopy (NIRS) to identify the composition and microstructure of a clay-based object has given the following results: Paligorskite, Leucite, Feldspar. The XRD results on the structure of iron oxide clay revealed the presence of Quartz, Muscovite, Anortite

⁴ Similarly as noted for the area of Mugnano in Teverina on the other bank of the Tiber, where the production included stamped bricks, tiles and mortaria, Gasperoni 2003, 37- 38.



172

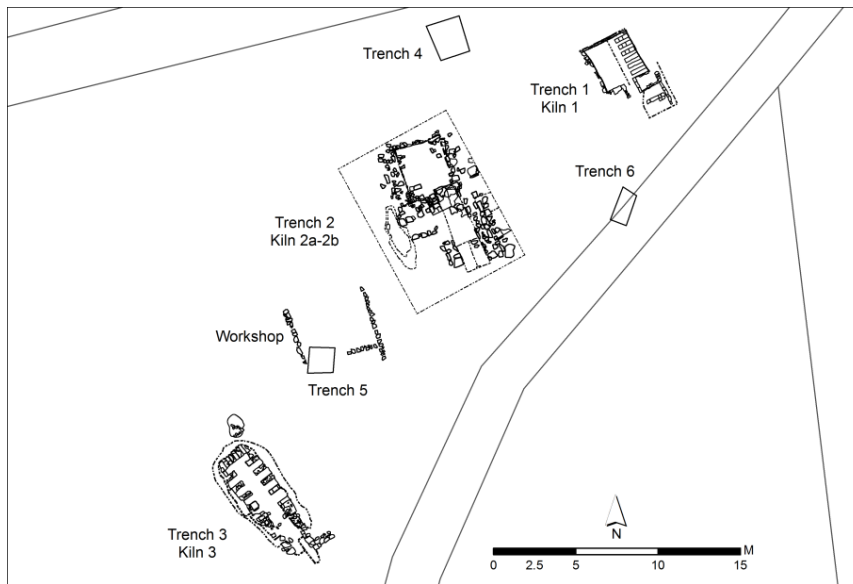
173 **Fig. 2:** Map of the site. The base map is courtesy of David Redhouse.

174

175 The excavation of the production centre at Montelabate concentrated on an area measuring
 176 25m by 30m on the top of the small hill (Fig.2). The study of the surface material indicated
 177 six defined areas for excavation which subsequently revealed three kilns, three dumps of
 178 material and a separate structure, possibly a workshop. Two of the kilns, which had the
 179 longest period of use, were located at the summit of the hill and oriented North-South,
 180 probably in order to create an updraft favourable for the firing process (Fig.3, Kilns 1 and 2).
 181 A third kiln was located further down the hill (Fig.3, Kiln 3) had the same orientation but
 182 with an elongated combustion chamber, probably in order to increase the forced draught. The
 183 kilns were all rectangular in shape with a double updraft chamber (the Cuomo di Caprio II/b
 184 typology (Cuomo di Caprio, 2007, 523-525, fig. 169), consisting of a lower combustion
 185 chamber with a stoking hole or *praefurnium*⁵.

186

⁵ For the description of the single structures see Ceccarelli *forthcoming*



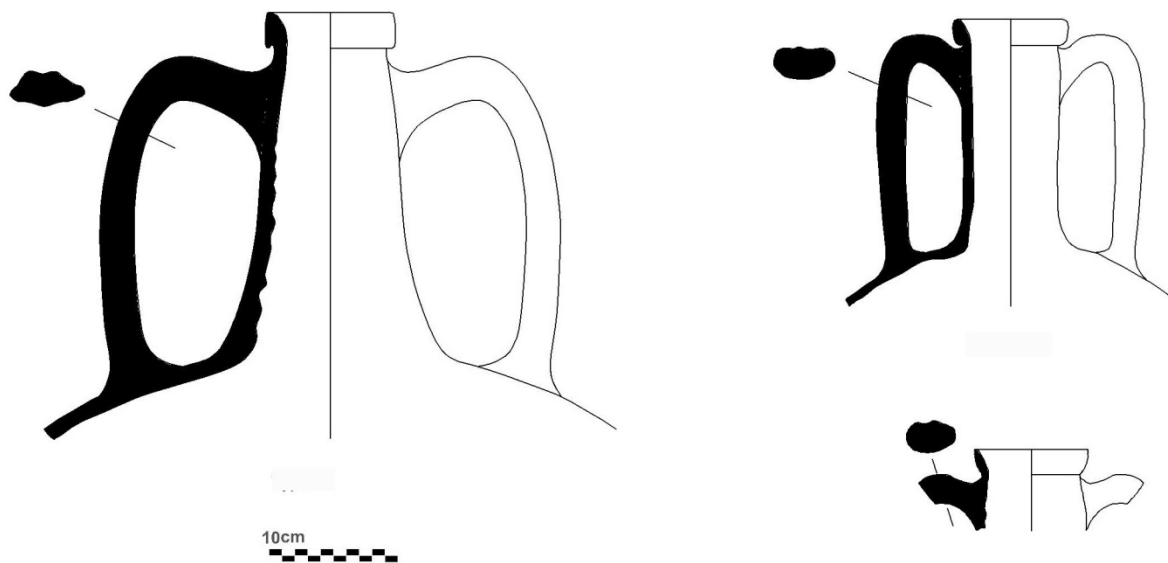
187

188 **Fig. 3:** Plan of the kilns identified during the excavation.

189

190 The kilns produced a type of flat-bottomed amphorae. It is labelled as the ‘Spello’ type after
 191 the name of the site where its production was identified for the first time. In the context of
 192 Ostia it is classified as Ostia III, 369-370 / II, 521 ((Panella, 1989, 143-146), Rizzo 2014,
 193 130), while the examples from the Upper Tiber valley have been called ‘Tiberine’ and
 194 ‘Altotiberine’⁶. The production of Montelabate revealed that there was little standardisation,
 195 as seven different types were identified with everted band rims (type 2.3-2.4 (Lapadula,
 196 1997)), tapered rims (type 2.5 of (Lapadula, 1997)) and rounded rims (type 4.10 of
 197 (Lapadula, 1997)) with diameters between 7.5cm and 9 cm. (Ceccarelli, *forthcoming*) (Fig.
 198 3).

⁶ (Molina Vidal, 2008), 227-229.



199
 200 **Fig. 4:** Example of amphorae found at Montelabate.

201
 202 These small wine amphorae, made from the Tiberian-Claudian period until the end of the 2nd
 203 century AD, were transported by river from the Upper Tiber valley to Rome and Ostia (see
 204 the recent analysis of Rizzo 2014). The local wine was the *Hirtiola*, as mentioned by Pliny
 205 (N.H. 14.37), that was exported from the Upper Tiber valley to Rome, the largest market, and
 206 Ostia. In Rome this type of amphorae represented the largest Italian production after the
 207 Dressel 2-4 from the Flavian period (see Ceccarelli *forthcoming*).

208 The kilns were also used to produce tiles and courseware, providing evidence for a local
 209 production system that continued in the late antique period, with production and consumption
 210 evidence until the 5th century AD.

211
 212

213 **3 – METHOD OF ANALYSIS**

214
 215 For the XRF analysis both kiln wastes and discarded failed products were selected: these
 216 artefacts were not suitable for the wine trade as they were either over-fired, under-fired or
 217 fractured amphorae⁷. The process of over-firing clay objects involved too higher temperature
 218 or too long a period of firing resulting in a ‘vitrification’ of the surfaces (ideal firing
 219 temperature was between 700 and 900°C). On the other hand the under-firing process

⁷ Similarly, as discussed for the courseware production at Scoppieto (Peinado Espinosa, 2015).

220 produced a failed sintering, resulting in a soft porous surface. Another type of failed product
221 were fractured ceramic vessels that did not withstand the thermal shock of cooling ((Cuomo
222 di Caprio, 2007, p.499).

223 A selection of 38 samples were analysed representing the main diagnostic groups of
224 amphorae, in addition to these groups are 12 samples of the same type of amphorae from
225 other sites in order to compare different productions. As previously noted, the amphorae were
226 distributed either by river and by land, therefore in order to test the method for a large
227 distribution network amphorae from the river harbour at Ardea and an inland site, such as
228 Segni, both in the area south of Rome were sampled. These sites which are distant from the
229 workshop are useful to explore the distribution of vine and amphorae from Umbria. A
230 programme of sampling fragments of amphorae discovered in the surrounding area with a
231 5km radius is currently on-going to determine the local distribution of the amphorae produced
232 in the workshop of Montelabate.

233

234 The pXRF spectra were collected using a Bruker Tracer IIIDS instrument. The
235 following settings have been used as the default choice: 40 keV and 10.70 μ A. Each spectrum
236 was collected for 30 seconds fixed time, following preliminary optimisation.

237 At the start of the process a reproducibility check was conducted by collecting at least
238 three spectra at the same sample point. Depending on the sample geometry, by default each
239 sample was analysed on one or more external surfaces and in one or more internal sections.
240 Possible differences in section and external surface compositions may be ascribed to the
241 production and firing process (e.g. external coating, combustion gas and ash, etc.).

242 The pXRF proprietary software was used for the peaks identification and to collect
243 raw intensity data. A customise database was then developed to extract intensity from the raw
244 spectra and to analyse them, as described below.

245 Quantitative data have been obtained by means of an innovative calibration. As
246 described in the following section, for which commercial feldspars and clays with variable
247 and certified composition as an internal standard for calibration were selected.
248 Standardisation has been carried out by linear regression of net peak intensity for selected
249 elements vs. composition (expressed as element or element oxide wt%) in each calibration
250 sample.

251

252

253
254
255
256
257
258
259
260
261
262
263
264
265
266
267
268
269
270
271
272
273
274
275
276
277
278
279
280
281

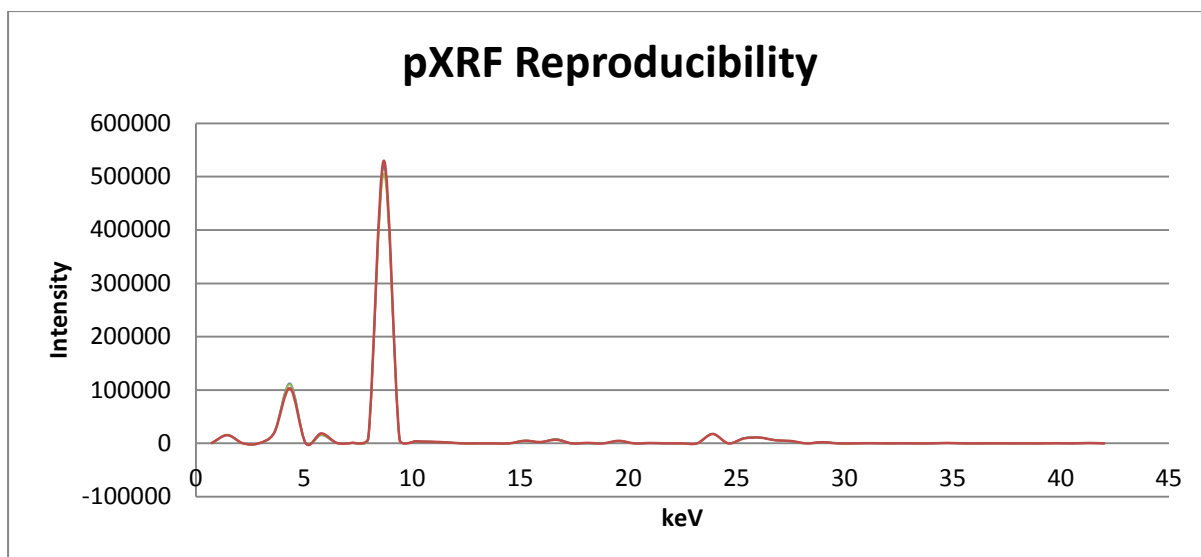
4 – RESULTS AND DISCUSSION

4.1. The sampling method

The potters of Montelabate mainly used a source of natural clay deposits as most of the products were made of a non-calcareous iron clay matrix tempered with mica and quartz, as identified in some samples which were thin sectioned. A further element to take into account when sampling amphorae is the different formation methods: parts of the vessel, such as handles and necks were produced separately and added to the main vessel by wiping that may result in small differences in the matrix on the surface. Therefore, the sampling strategy involved analysing both surfaces and sections in order to detect variations. Samples were accurately prepared to avoid any chemical contamination, as suggested also in Hunt-Speakman (Hunt and Speakman, 2015, 627) and each fragment was sampled by six readings on average.

A critique that has been made of the use of pXRF on clays is the difficulty in determining compositional profiles for the lack of reproducibility and standard calibration. To test and overcome this potential problem, a study has been undertaken to test the performance of pXRF as for repeatability and reproducibility of the measurements.

The results illustrated in Fig. 5 show an example of spectra reproducibility, including seven different analyses repeated on the same object section, collected over the course of a two days period. Through an analysis of the overlapping curves, the incidence of the standard deviation was examined for each value with respect to the average of the population, as well as considering each single peak. An overall difference of $\pm 3.5\%$ was obtained for the peak intensity. Similar values were achieved when comparing peak area.



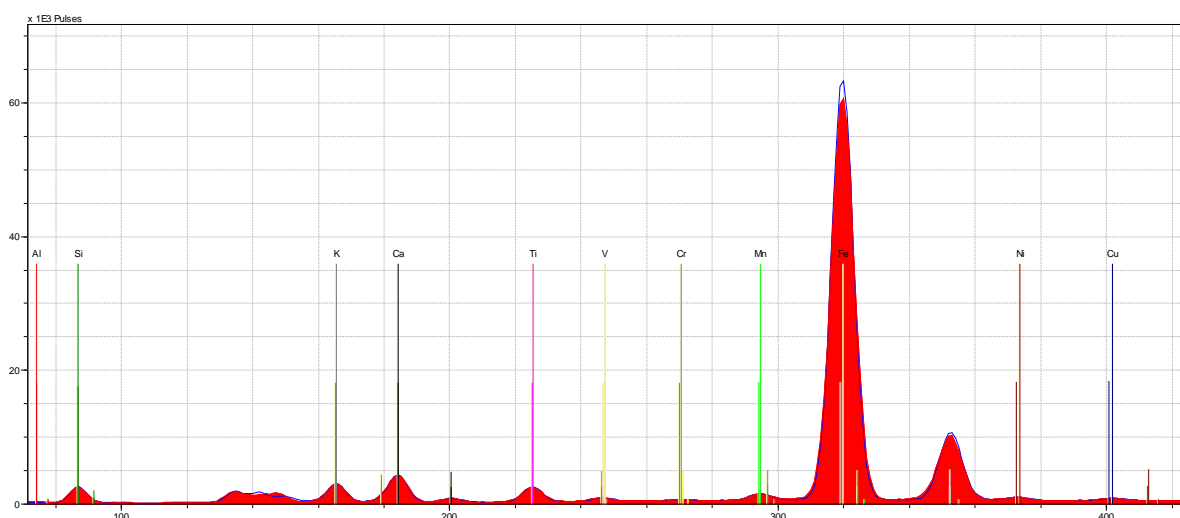
282
283

284 **Fig. 5:** Example of spectra reproducibility.

285 Through the extraction of the net intensity data, it can be noted that the most intense peaks
 286 are K, Ca and Fe (Fig.6a), which were also characterised by a broad variation of intensity,
 287 besides Si and Al which have low net intensity due to poor instrumental response to very
 288 light elements. In terms of the minor elements, Fig.6b shows that some are characterised by
 289 limited variations of peak intensity, others, such as Sr, Mn and Ti by a much broader gradient
 290 of concentration in the examined dataset.

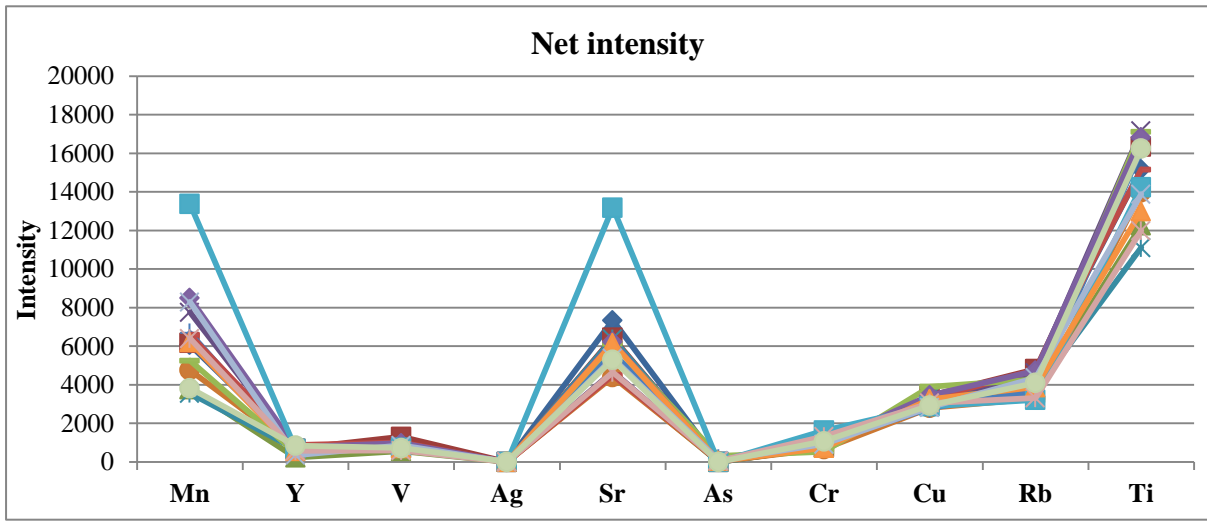
291 **Fig.6:** Net peak intensity for some representative elements. a) Significant elements peaks
 292 (K α peak); b) Net intensity of minor elements in different samples of the dataset.

293 a)



294

295 b)



296

297

298 In order to develop a robust method to fingerprint clay production, analysis was also
299 compared the relative intensity of each element signal with respect to that of a reference peak.
300 This procedure overcomes the possible variation of the overall intensity of the spectrum due
301 to any instrumental or external reason. Abundant and scarce elements were considered
302 separately in two distinct groups.

303 The representative samples of the dataset evidenced a marked variation of intensity ratio with
304 respect to a reference element depending: a) on the selection of sections or external surfaces;
305 b) on the provenience of the sample, as presented in paragraph 4.3.

306

307 4.2. Calibration

308

309 The aim of this work was to set up a fingerprinting method to assess the composition and
310 origin of ceramic objects. This process could simply rely on peak intensities (absolute or
311 relative). However, a quantitative analysis is proposed here to allow direct comparisons with
312 literature, as far as it is consistent with the intrinsic limits of the technique for quantitative
313 analysis. In order to conduct the analysis the study did not rely on automatized calibration
314 algorithms provided with the instrument, due to the mentioned limitations of such calibration
315 procedures. Furthermore, statistical methods, such as that proposed by (Goren et al., 2011)
316 were not applied. Instead, several natural clay samples were identified, with a similar
317 qualitative composition with respect to the collected ones. Different commercial samples of

318 feldspars and clays were collected, with a variable composition certified by two different
 319 producers, to be used as standards. This procedure allowed the comparison of samples with
 320 the same matrix as the analytes, therefore limiting as much as possible the matrix effect
 321 limitations. A further advantage is that commercial samples represent a suitable comparison
 322 to check the reproducibility of the method in different laboratories.

323 The obtained calibrating curves were used to calculate the following composition
 324 (Table 1).

Sample	Element (wt%)					
	K	Al	Ca	Fe ₂ O ₃	Si	Ti
A1	2.275	16.756	8.469	5.606	40.033	0.501
A2	2.535	17.311	9.934	5.566	27.276	0.489
A3	2.369	15.694	2.249	7.122	19.599	0.679
A4	2.425	18.235	3.186	7.709	21.926	0.646
A5	2.452	14.631	9.899	5.606	31.375	0.429
A6	2.250	14.470	9.615	4.914	30.191	0.427
A7	2.686	17.680	2.358	5.971	24.874	0.598
A8	1.543	14.400	1.206	5.568	20.202	0.528
A9	2.173	22.254	3.030	6.936	40.747	0.683
AT1	2.362	16.271	5.724	5.951	33.049	0.506
M1	1.979	17.195	2.063	8.109	25.978	0.816
M2	2.128	23.594	5.069	6.897	51.220	0.638
M3	2.035	16.964	2.225	7.758	35.794	0.739
M4	2.104	17.865	4.262	7.492	36.938	0.739
M5	0.479	9.272	0.966	2.237	0.000	0.203
M6	0.453	10.104	2.217	1.868	0.000	0.138
M7	2.692	19.321	4.529	8.247	33.449	0.756
M8	2.076	15.925	6.125	5.830	35.545	0.510
M9	1.713	15.139	1.266	5.048	6.829	0.433
M10	1.444	16.087	3.042	5.590	10.216	0.480
M11	1.918	16.294	5.347	5.688	36.108	0.518
M12	2.237	17.357	4.111	7.014	31.075	0.692
M13	2.074	15.948	4.747	6.449	38.381	0.591
M14	1.924	17.911	4.890	6.852	36.173	0.629
M15	1.272	14.031	2.847	5.215	13.366	0.497
M16	1.654	13.846	1.746	5.569	18.344	0.534
M17	1.783	16.410	7.917	5.196	25.642	0.456
M18	0.939	9.341	2.379	4.647	3.975	0.374
M19	2.329	17.311	1.277	7.555	32.453	0.682
M20	1.397	14.770	1.754	6.120	10.223	0.585
M21	2.169	16.433	3.883	7.358	31.458	0.608
M22	1.227	17.565	3.367	5.520	15.537	0.487

M23	2.253	21.700	2.006	6.915	39.127	0.638
M24	1.826	17.403	5.066	5.409	30.094	0.486
M25	2.406	19.182	2.727	8.348	50.271	0.713
M26	1.979	20.684	3.202	7.447	28.160	0.683
M27	0.518	14.677	1.279	2.717	0.000	0.278
M28	1.832	13.823	6.215	4.593	18.030	0.433
M29	2.015	13.130	5.313	6.372	34.264	0.528
M30	1.881	15.902	4.582	6.287	26.901	0.541
M31	1.202	11.582	2.114	3.713	7.781	0.335
M32	2.036	14.262	3.442	6.664	29.160	0.580
M33	1.555	17.588	2.381	6.108	17.016	0.495
M34	1.805	15.925	3.101	6.494	22.305	0.573
M35	1.307	14.031	2.455	3.590	19.823	0.359
M36	1.793	20.291	3.321	6.970	38.345	0.662
M37	1.428	12.136	3.445	4.606	9.047	0.380
M38	2.143	18.628	2.935	6.410	37.598	0.687
S1	1.577	12.136	7.561	8.815	29.037	0.468
S2	1.412	13.638	5.811	8.130	17.222	0.437

325

326

327 **4.3. Fingerprinting the Montelabate amphorae**

328

329 The net intensity of the XRF peaks of different elements was extracted for each sample which
330 allowed the identification of the relative composition through the reported calibration curves.
331 The following elements have been recognized in every sample: Al and Si are abundant in
332 clay composition, but light elements are poorly detected unless operating under vacuum.
333 Therefore, low intensity peaks are usually obtained, especially for Al. K and Ca were
334 abundant elements, as expected, with intense peaks showing marked variability with
335 provenience and surface analysed (external surface or internal section).

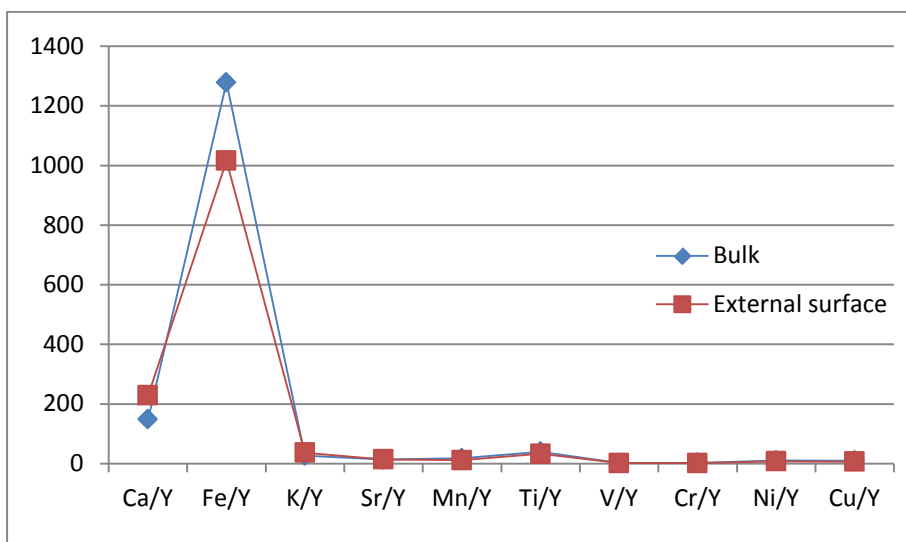
336 Ti, V, Cr and Mn were minor peaks usually correlated to Fe, in particular Ti, the attribution
337 of the latter is relatively uncertain being very similar to the escape peak (ESC) of Fe. Mn
338 showed some variability, also correlated with colour. Fe was the most intense peak, showing
339 wide variations depending also in this case from provenience, type of clay and the analysed
340 section. Ni, Cu and Zn were minor elements without any significant features for the purposes
341 of fingerprinting. Rb, Sr, Y and Zr were regularly present. The former was not considered
342 significant due to similarity with the sum peak of Fe. Furthermore, Y and Zr did not vary

343 appreciably. By contrast Sr was very sensitive to the geographic provenience of the amphorae
344 and or fabric.

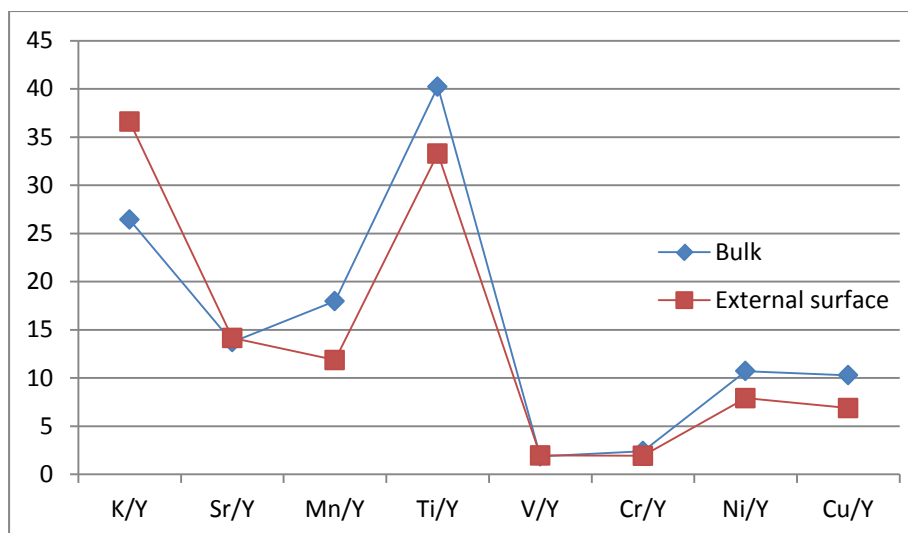
345 The net intensities of each significant element's peak were extracted in order to
346 compare them systematically to achieve fingerprinting of the Montelabate production. In the
347 database, the raw dataset was recorded in terms of the object type, provenience and sampling
348 date. The extracted data were automatically elaborated as intensity ratio between selected
349 elements or ternary groups for multivariate analysis. In the database, the most significant
350 elements identified for the fingerprint of the Montelabate production were selected in order to
351 determine the elements ratio on the external surface and sections of the samples, i.e. K, Ca,
352 Fe, Sr, Mn, Ti, V, Cr, Ni, Cu were factored by Y, Zr, Fe or Ca. The results were plotted using
353 simple binary or ternary diagrams.

354 The section of every sample was richer in all the elements with the exception of K and
355 Ca. The two latter elements were more abundant on the surface, possibly as a result of the
356 firing process or due to the secondary deposition in the kiln in the dump of ash. To confirm
357 this hypothesis, analysis was also made of some of the samples of ancient raw clay used as
358 daub in the Etruscan settlement of Col di Marzo, excavated close to the area of the Roman
359 kilns. The results reveal a perfect overlapping of the spectra confirming that the chosen
360 elements were part of the raw clay for the amphorae production and not added as temper by
361 the potter. Therefore, this method of elements internal ratio analysis has proved consistent to
362 fingerprint any given ceramic production and the optimal results were achieved on sections.

363 **Fig. 7:** Example of representation of samples composition based on elements ratio. The
364 composition is compared between the external surface and an internal section or bulk.



365



366

367

368 This method proved useful for clustering the different groups of amphorae (a similar
369 approach was used on clay cuneiform tablets by (Goren et al., 2011)).

370 In order to understand which elements are correlated between each other, correlation matrixes
371 were built, which can be exemplified by the following examples and graphics (Fig.8). The
372 average peak intensity $I_{i,av}$ (or composition if rielaborated through the calibration curves) of
373 every element has been calculated for a given set of objects, e.g. amphorae, section,
374 Montelabate site by averaging out the single net intensities of that element's peak for every
375 sample (I_i). ΔI_i has been calculated as:

376
$$\Delta I_i = I_i - I_{i,av}$$

377 Correlation plots collect ΔI_i vs. ΔI_j valued for the selected object, i and j being two different
378 elements. By focusing on section samples of Montelabate's amphorae, the following
379 correlation plots require discussion.

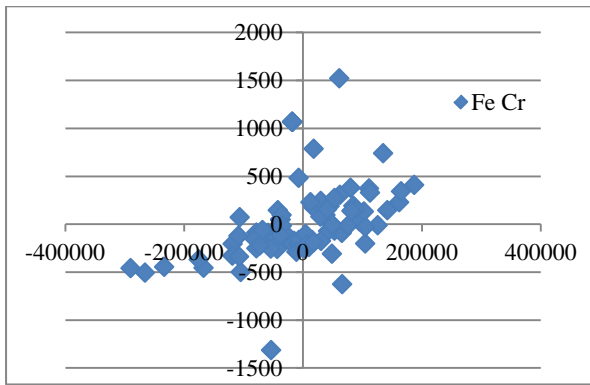
380 When plotting ΔI_{Fe} vs. ΔI_{Cr} (Fig. 8a) it is possible to observe that Fe and Cr increase at once.
381 The same can be concluded for other elements, such as Fe with V, Y, Co (Fig. 8b-d), Cu, Ni
382 (Fig. 8e,f), Ti (although very near to the *esc* peak of Fe, Fig. 8g), K (Fig. 8h).

383

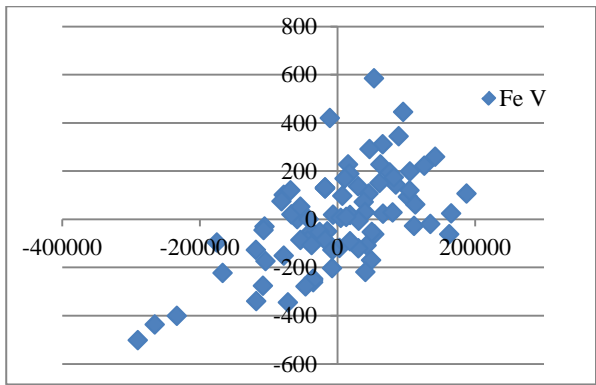
384

385 **Fig. 8:** Examples of correlation plots between Fe and other elements. ΔI_{Fe} reported on the x-
386 axis in correlation with a) ΔI_{Cr} ; b) ΔI_V ; c) ΔI_Y ; d) ΔI_{Co} ; e) ΔI_{Cu} ; f) ΔI_{Ni} ; g) ΔI_{Ti} ; h) ΔI_K .

387 a)

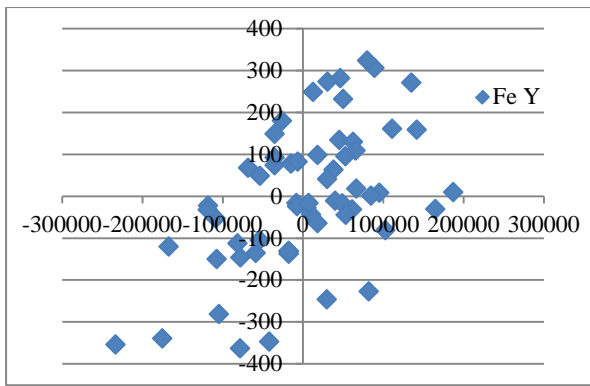


b)

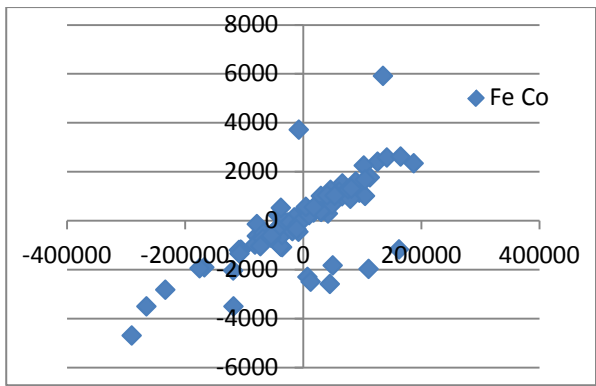


388

389 c)



d)

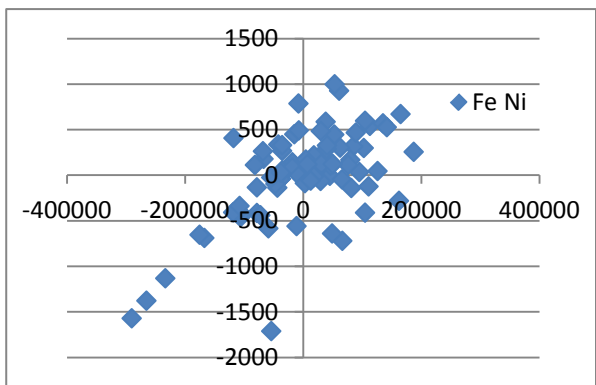
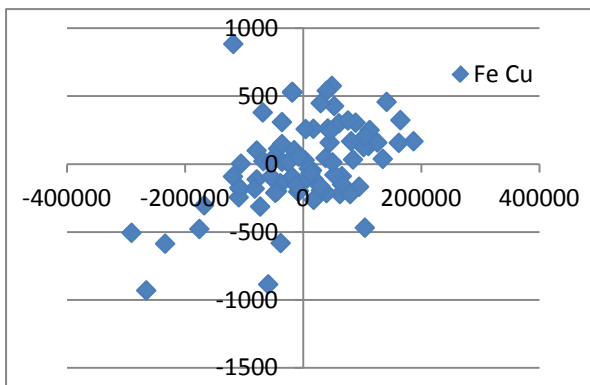


390

391 e)

f)

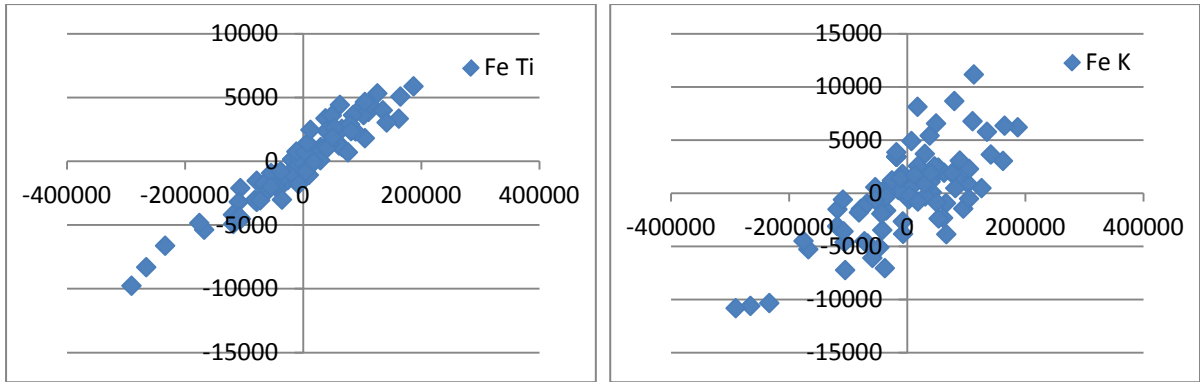
392



393

394 g)

h)



395

396

397 Conversely, other elements do not seem correlated between each other. For instance, looking
 398 at ΔI_{Fe} , it seems rather independent from Ca (Fig. 9a), which is often reported as added to the
 399 fabric⁸. Additionally, Fe does not seem correlate to a signal at 10.5 keV circa, which may be
 400 indicative of the presence of As (line K) or Pb (line L) (Fig. 9b). The latter interpretation is
 401 supported here, since Pb could be pollution in the clay refinement. Accordingly, Mn and Fe
 402 or Cr are not correlated⁹ (Fig. 9c,d).

403

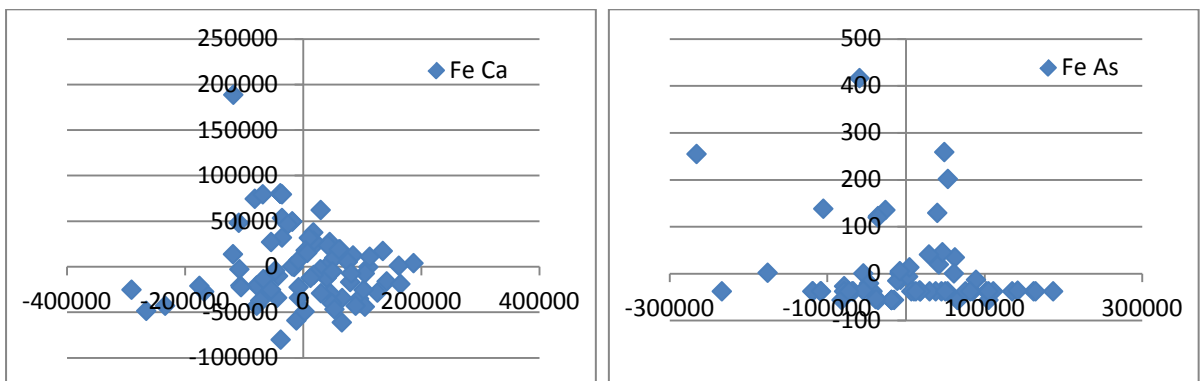
404

405

406 **Fig. 9:** Correlation plots between a) ΔI_{Fe} and ΔI_{Ca} ; b) ΔI_{Fe} and $\Delta I_{As/Pb}$; c) ΔI_{Ca} and ΔI_{Cr} ; d)
 407 ΔI_{Mn} and ΔI_{Cr} .

408 a)

b)

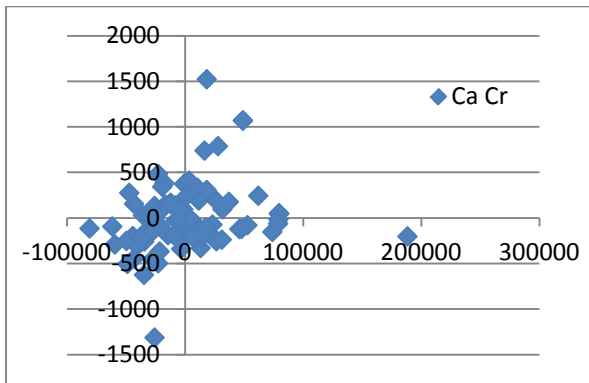


409

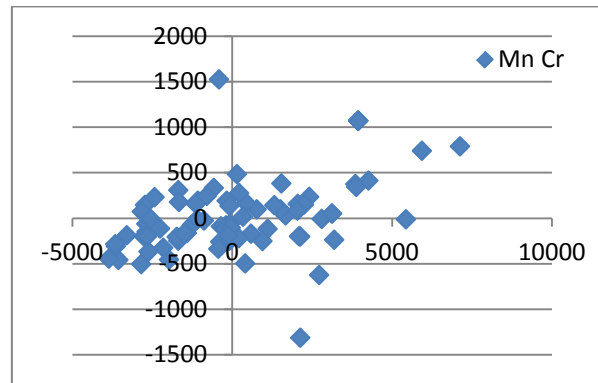
⁸ For instance at Scoppieto in Umbria, for coarseware production it was employed a clay with high content of calcite (Calcium carbonate $CaCO_3$) with a percentage higher than 7-8% (Peinado Espinosa, 2015, 59).

⁹ Although (Hunt and Speakman, 2015, 367), suggest that for Cr can only be performed a semi-quantitative analysis of archaeological ceramics, as the pXRF is not reliable for this element.

410 c)



d)



411

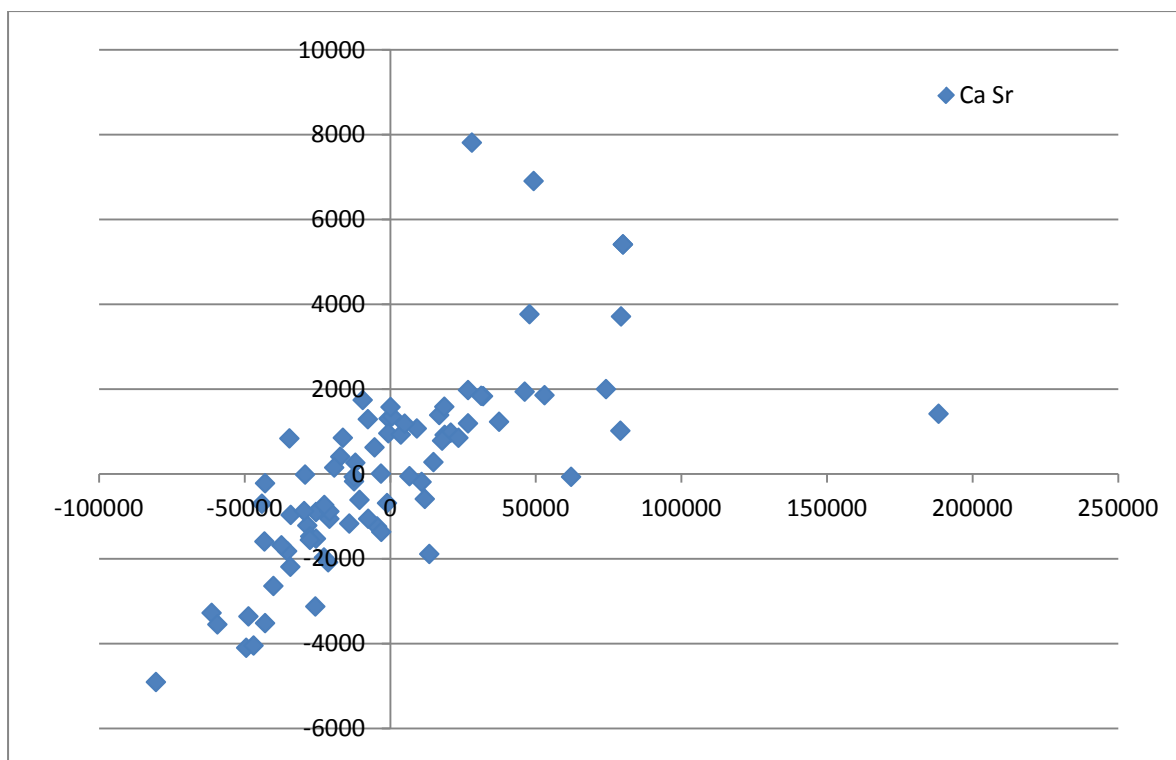
412

413 Based on these considerations we have identified a set of elements, Fe/Y/K/Cr with a highly
414 correlated concentration between each other in the Montelabate amphorae, which can
415 represent the typical composition of the local clay used for production. Other elements, such
416 as Ca and Pb, can be identified as typical of the Montelabate fabric. It is also possible to
417 identify Sr as a minor element with an interesting variability. It did not seem correlated to the
418 clay components, but predominantly to Ca (Fig. 10). Therefore, it can be interpreted as an
419 alkali-earth impurity of the Ca-based additive used during manufacturing.

420 The future research will focus on sampling coarseware production as well as the raw clay at
421 Montelabate. Concurrently, a representative selection of fragments have also been subject to
422 petrographic analyses. The preliminary results of the study of the amphorae of Montelabate
423 revealed a coarse grain texture characterised by oxide clay groundmass with a mineralogical
424 composition consisting of angular and subangular quartz, crystallised volcanic rock, mica and
425 feldspar.

426

427 **Fig. 10:** Correlation plot between ΔI_{Ca} and ΔI_{Sr} .



428

429

430 4.4. Comparison with amphorae from different sites.

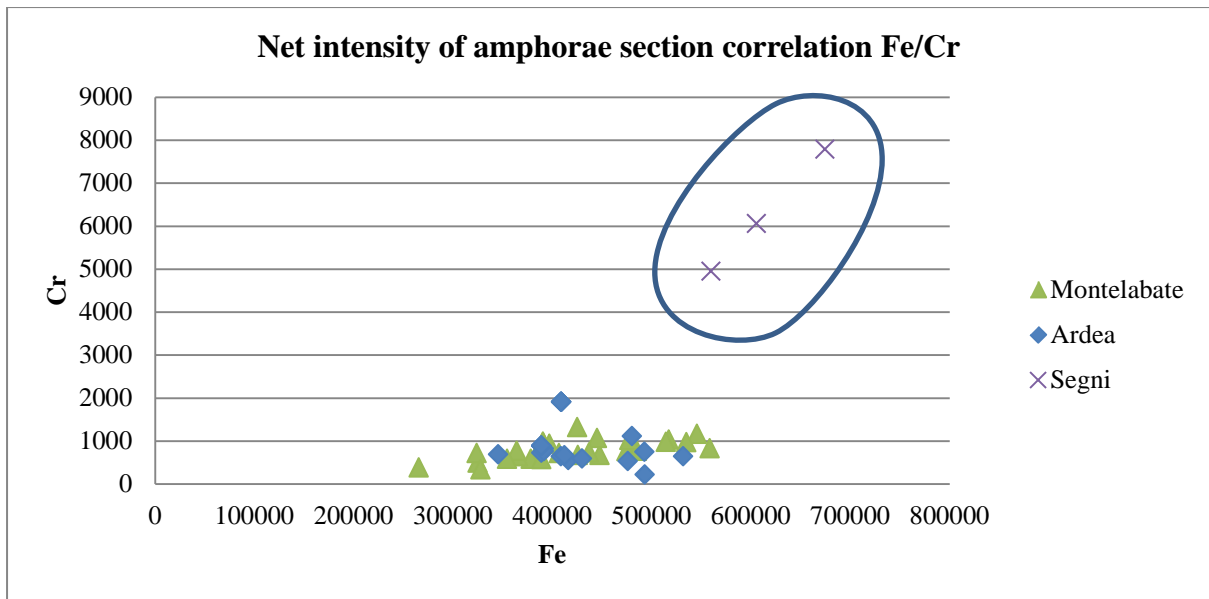
431

432 In order to validate the results, the selected element intensity ratios based on amphorae
 433 provenience were clustered to fingerprint the production in the area of Montelabate of
 434 amphorae, found in different sites.

435 As discussed above, some elements were attributed to the natural clay, others such as Ca, Sr
 436 and Pb to manufacturing. By comparing the net intensity and intensity ratio between couples
 437 of elements, indicators of local production were searched. A first example was formed by Fe
 438 and Cr, which are attributed to the clay composition. Fig. 11 reports the Fe/Cr peak intensity
 439 ratio for amphorae found in different sites considering the sections (a) and external surfaces
 440 (b). It is evident that for the whole samples list from Montelabate, the values varied between
 441 ca. 250 and 750. Samples found in Ardea were partly included in the given intensity ratio,
 442 partly not (higher and lower values), whereas the samples found in Segni definitely did not
 443 match the intensity ratio range identified in the Montelabate site. The same method was
 444 applied to other significant intensity ratios, such as K/Cr (Fig. 12)

445

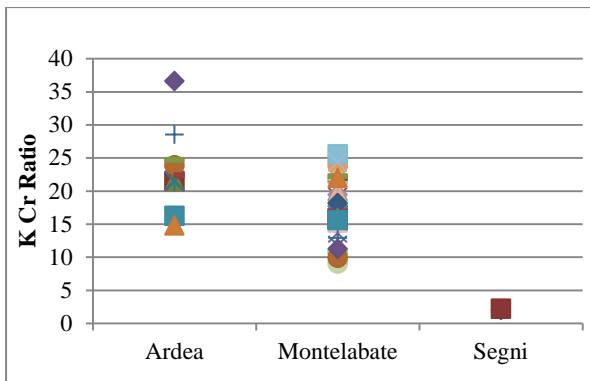
446 **Fig. 11:** Fe vs. Cr peak intensity ratio for amphorae found in different sites. Sections only .



447

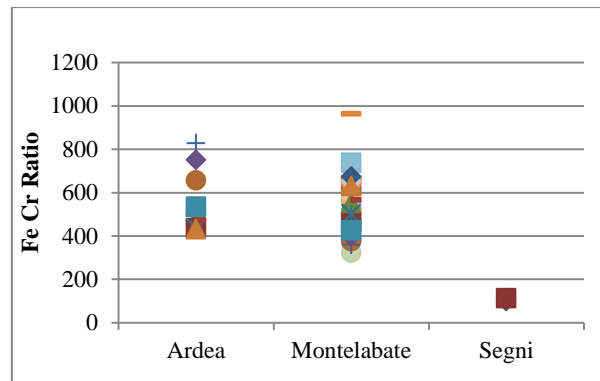
448 **Fig. 12:** Significant element intensity ratios clustered by site: a) K/Cr, section; b) Fe/Cr, section;
 449 section; c) Fe/Cr external surface; d) Ca/Cr, section; (e) Ca/Cr, external surface, f) Mn/Cr,
 450 section.

451 a)



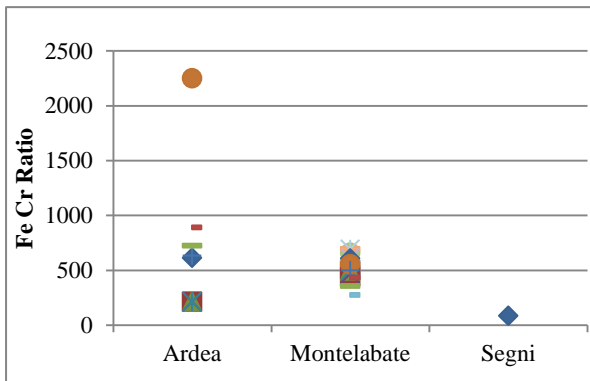
452

b)



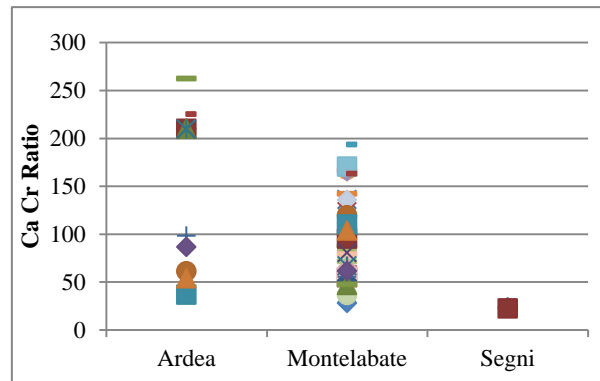
453

454 c)

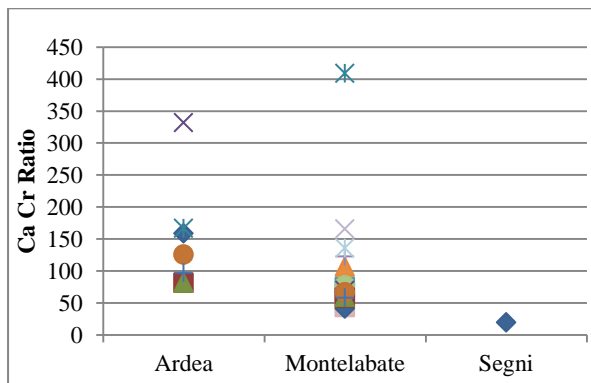


455

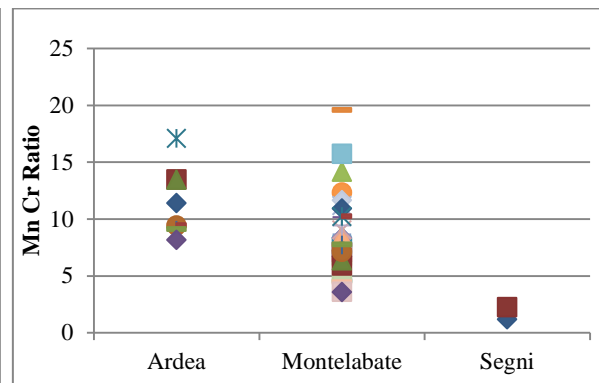
d)



456 e)



f)



457

458

459 Applying this method it is possible to identify a specific composition trend for the amphorae
460 from Montelabate, characterised by clustered values of the intensity ratios of relevant
461 elements. Some of them were typical of the clays used for ceramics production, other
462 elements were added during manufacturing.

463 Therefore, by considering only the ratio between peak intensities it is possible to distinguish
464 the main components which characterise the Montelabate production and to obtain a possible
465 composition range which enables the distinction of amphorae produced in this site from other
466 production areas. This represents a solid methodology as it is independent from the
467 availability of the calibration standards, the spectra collection parameters and all those factors
468 influencing the peak intensity of a single element.

469

470 5. CONCLUSION

471

472 The research presented in this paper aimed to develop an application of a non-destructive
473 analytical method of clay analysis by portable X-ray fluorescence (pXRF). The innovative
474 methodology proposed in this project to fingerprint any given ceramic production is based on
475 the quantification of the internal ratio of the peaks area that when the values are constant
476 indicate a similar composition.

477 This method is based firstly on the qualitative interpretation of the principal elements of each
478 single spectrum and then, in a customised database, the intensity ratio of the elements is
479 correlated to overcome the limits of each single reading. It allows identifying correlated
480 peaks through a correlation matrix. Couples of elements that have significant variation are
481 used as indicators of fabric nature, provenance and composition. For quantitative analysis,

482 due to the lack of “off-the-shelf” calibration standards for ceramics, feldspars and clays with
483 known composition were used to calculate the absolute amount of the components.

484 Applying this method has been possible to identify the local production of the
485 Montelbate workshop, even if the amphorae fragments revealed many differences in the
486 fabrics: some samples having a red fabric, hard when properly fired but generally the surfaces
487 are soft and porous. The surface and breaks have the same colour and occasionally the grey
488 core suggests an uneven firing temperature. Several examples have a hard grey vitrified
489 surface. Other samples present a more refined reddish-yellow fabric. The surface is lighter in
490 colour than in the breaks. Therefore, both morphologically and in colour of fabric the
491 Montelabate amphorae differ greatly, however the chemical analyses have proved that they
492 are produced with similar clay and temper.

493 The results have important archaeological implications because the kilns that have
494 been excavated at Montelabate are the only certain site for the production of the flat bottomed
495 wine amphora in the *Regio VI* (Umbria) and by assessing the technology of its production, it
496 offers a model to study the ancient economy and the network of exchange, identified by a
497 scientific method.

498

499

500 **AKNOWLEGMENT**

501

502 A special thanks to the McDonald Institute for Archaeological Research, University of
503 Cambridge and Department of Chemistry, Università degli Studi di Milano for the use of the
504 equipment and the laboratory.

505 We are really grateful to Dott. Francesco Di Mario and Dott. Alessandro Betori,
506 Soprintendenza Archeologia del Lazio e dell’Etruria Meridionale for granting the permission
507 to conduct the analysis on the sites of Ardea and Segni.

508 Fundamental is the support of Dott. Davide Maccaferri, Sibelco, Viale Dino Ferrari, 75/83,
509 Maranello (MO), Italy, and of I.MA.F. SPA, Via Mulino Dionigi n. 2, Dorgola di Carpineti
510 (RE), Italy, for providing their calibrated feldspars, sands and clays to test the instrument
511 calibration.

512

513

514

515 **REFERENCES**

- 516 Attaelmanan, A.G., Mouton, M., 2014. Identification of archaeological potsherds excavated
517 at Mleiha using XRF. *J. Archaeol. Sci.* 42, 519–524. doi:10.1016/j.jas.2013.12.001
- 518 Attema, P.A.J., Beijer, A.J., Kleibrink, M., Nijboer, A.J., van Oortmerssen, G.J.M., 2003.
519 Pottery classifications: ceramics from Satricum and Lazio, Italy, 900 - 300 BC.
520 *Palaeohistoria* 43/44, 321–396.
- 521 Ceccarelli, L., *forthcoming* Production and trade in Central Italy in the Roman period. The
522 amphorae workshop of Montelabate in Umbria. *Papers of the British School at Rome*.
- 523 Conrey, R.M., Bettencourt, N., Seyfarth, A, Hoose, a Van, Wolff, J. A., 2014. Calibration of
524 a portable X-ray fluorescence spectrometer in the analysis of archaeological samples
525 using influence coefficients. *Geochemistry Explor. Environ. Anal.*
526 doi:10.1144/geochem2013-198
- 527 Cuomo di Caprio, N., 2007. *Ceramica in archeologia 2: Antiche tecniche di lavorazione e*
528 *moderni metodi di indagine*. Roma: Erma di Bretschneider.
- 529 Donnini, L., Rosi Bonci, L., 2008. Civitella d’Arna (Perugia, Italia) e il suo territorio. Carta
530 archeologica. Oxford, BAR international series.
- 531 Frahm, E., Doonam, C.P., 2013. The technological versus methodological revolution of
532 portable XRF in archaeology. *J. Archaeol. Sci.* 40, 1425–1434.
533
- 534 Gasperoni , T. 2003, *Le fornaci dei Domitii. Ricerche topografiche a Mugnano in Teverina,*
535 *Daidalos, Studi e e ricerche del Dipartimento di Science del Mondo Antico, Viterbo*
- 536 Goren, Y., Mommsen, H., Klinger, J., 2011. Non-destructive provenance study of cuneiform
537 tablets using portable X-ray fluorescence (pXRF). *J. Archaeol. Sci.* 38, 684–696.
538 doi:10.1016/j.jas.2010.10.020
- 539 Hunt, A.M.W., Speakman, R.J., 2015. Portable XRF analysis of archaeological sediments
540 and ceramics. *J. Archaeol. Sci.* 53, 626–638. doi:10.1016/j.jas.2014.11.031
- 541 Lapadula, E., 1997. Le anfore di Spello nelle Regiones VI e VII. *Papers of the British School*
542 *at Rome* 65, 127–156.
- 543 Malone, C., Stoddart, S., 1994. *Territory, Time and State. The archaeological development of*
544 *the Gubbio basin*, Cambridge, Cambridge University Press.
- 545 Molina Vidal, J., 2008. Mercantile trade in the Upper Tiber valley: the villa of Pliny the
546 Younger “in Tuscis,” in: Coarelli, F., Patterson, H. L. (eds.) *Mercator Placidissimus.*
547 *The Tiber Valley in Antiquity: New Research in the Upper and Middle River Valley:*
548 215–249.
- 549 Panella, C., 1989. Le anfore italiche del II secolo d.C., Le anfore italiche del II secolo d.C., in
550 *Amphores romaines et histoire économique, dix ans de recherche. Actes du colloque de*

- 551 Sienne (22-24 mai 1986), organisé par l'Università degli studi di Siena, l'Università
552 degli studi di Roma-La Sapienza, le Centre.
- 553 Peinado Espinosa, M.-V., 2015. Lo studio delle ceramiche comuni nel Mediterraneo
554 Occidentale e nell'Umbria, in M. Bergamini (a cura di), Scoppieto V, I materiali.
555 Ceramiche comuni, Roma Edizioni Quasar.
- 556 Rizzo, G. 2014, Le anfore, Ostia e i commerci mediterranei in Rizzo, G., Panella, C.
557 (eds). *Ostia: VI, Le terme del nuotatore. I saggi nell'area NE*. Roma: "Erma" di
558 Bretschneider, 67-440.
- 559 Schackley, M. S. 2011. An Introduction to X-Ray Fluorescence (XRF) Analysis in
560 Archaeology. In Schackley, M.S. (ed.), *X-Ray Fluorescence Spectrometry (XRF) in*
561 *Geoarchaeology*. Houten, Springer: 7-44.
- 562 Shugar, A. N. J. L. Mass, (eds.) 2014. *Handeld XRF for Art and Archaeology*. Leuven,
563 Leuven University Press.
- 564 Speakman, R.J., Little, N.C., Creel, D., Miller, M.R., Inanez, J.G., 2011. Sourcing ceramics
565 with portable XRF spectrometers? A comparison with INAA using Mimbres pottery
566 from the American Southwest. *J. Archaeol. Sci.* 38, 3483–3496.
567 doi:10.1016/j.jas.2011.08.011
- 568 Speakman, R. J., Shackley M.S. 2013. Silo Science and Portable XRF in Archaeology: A
569 Response to Frahm. *J. Archaeol. Sci.* 40, 1435-1443.
- 570 Stoddart, S.K.F., Baroni, M., Ceccarelli, L., Cifani, G., Clackson, J., Ferrara, F., della
571 Giovampaola, I., Fulminante, F., Licence, T., Malone, C., Mattacchioni, L., Mullen, A.,
572 Nomi, F., Pettinelli, E., Redhouse, D., Whitehead, N., 2012. Opening the Frontier: the
573 Gubbio – Perugia frontier in the course of history. *Papers of the British School at Rome*
574 80, 257–94.
575